

See discussions, stats, and author profiles for this publication at: <https://www.researchgate.net/publication/283490272>

# Low-Frequency Magnetic-Field Immunity Surface Scan Method

Conference Paper · August 2015

DOI: 10.1109/ISEMC.2015.7256307

---

CITATIONS

0

---

READS

26

2 authors, including:



[Mart Coenen](#)

EMCMCC, Breda, the Netherlands

21 PUBLICATIONS 184 CITATIONS

SEE PROFILE

All content following this page was uploaded by [Mart Coenen](#) on 04 November 2015.

The user has requested enhancement of the downloaded file. All in-text references [underlined in blue](#) are added to the original document and are linked to publications on ResearchGate, letting you access and read them immediately.

# Low-Frequency Magnetic-Field Immunity Surface Scan Method

Mart Coenen  
EMCMCC  
Breda, the Netherlands  
[mart.coenen@emcmcc.nl](mailto:mart.coenen@emcmcc.nl)

Bharat Kathari  
IBI Group  
India  
[bharatkathari@gmail.com](mailto:bharatkathari@gmail.com)

**Abstract** — Many sensor designs incorporating electronics are becoming more vulnerable to low frequency (LF) magnetic field (H-fields) when used in close proximity of electrically driven actuators, linear and rotating motors. The complex geometrical structure of the sensor's front-end design is often unknown. The sensor's front-end position is where the physical measurement quantity is transferred into an electrical quantity and then led up to the amplification stages. Again, given by the fact that low-frequency H-fields are hard to shield, the externally generated H-fields i.e. magnetic flux penetrates into the few sub-mm square area and induces interfering voltages:  $U = -d\phi/dt = -dB.A/dt$ .

At this moment, no formal H-field immunity requirements nor test methods exist which is applicable in the frequency range 10 Hz to 1 MHz.

To be able to characterize the LF H-field immunity of these sensors, a surface scan method has been developed by which local H-fields can be injected in the various orthogonal orientations over the surface of the sensor by which its most sensitive orientation and response can be visualized.

Knowing the absolute and orientation sensitivity of sensors can be useful in the selection process of sensors and will determine their fit-for-use prior to system integration.

**Keywords** — H-field, sensitivity, signal integrity, sensors, pre-system integration analysis

## I. INTRODUCTION

The use of a surface scanner to characterize RF emission and/or immunity is not new and many of those are commercially of the shelf (COTS) available. What is lacking are means to characterize i.e. quantify and qualify the LF H-field immunity performance of sensors system as there are no specific EMC requirements in a qualification process of sensor systems and other electronic subsystems used in close proximity of electrically driven actuators like solenoids, linear and rotating motors [1].

To enable LF H-field qualification of sensor systems, one first need to know the fields appearing near to the boundaries of those often used solenoids, linear and rotating motors. Even the present static magnetic fields e.g. resulting from permanent magnet motors combined with fast rotation, movements and acceleration results in flux variations:  $d\phi/dt$ .

An everlasting challenge to go from metal frames to lighter carbon-fiber and other non-conductive material frames and structures diminishes any H-field shielding between the actuator and sensor to nil. It is even considered to make motor housings from carbon-fiber and other non-conductive material to lower the nearby eddy-current losses in the carrier frame of the motor.

A cost-effective approach is to incorporate the actuator drive electronics and its encoder or sensor system together with the actuator to eliminate filtering and expensive shielded cables for the signals in-between, such that only filtering at the drive's supply input remains necessary.

What is known over centuries is that even static H-fields can already degrade or diminish permeability of inductor core materials by orders of magnitude which then results in e.g. a time-dependent power conversion efficiency of DC/DC-converters or time-dependent filtering performance of compact signal and supply filters, see figure 1.

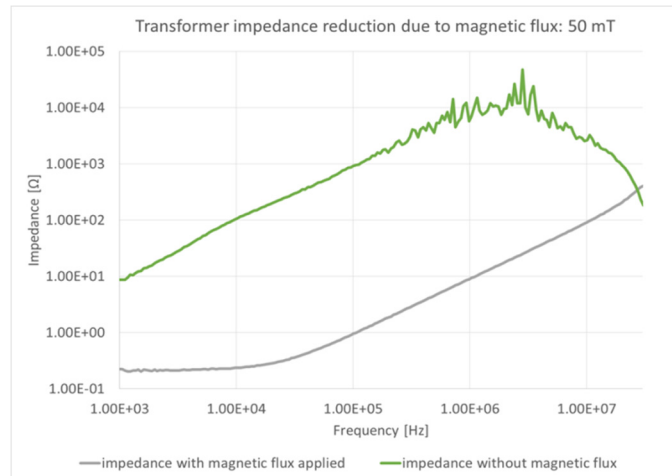


Figure 1 - Transformer inductance degradation due to magnetic flux

## II. PRE-REQUISITE

To be able to characterize the LF H-field immunity of sensor and other subsystems by surface scanning, a means to generate sufficient flux or H-fields locally will be necessary, when possible in three orthogonal orientations with small aperture [2].

The design of an audio recording head as used with magnetic tape recordings is considered. With such a tape head structure local H-fields can be generated over the gap of the recording head's core, see figure 2. Such a recording head, a round core with a gap or double C-core with a single slit, is provided with a number of windings through which an LF-current is driven. This structure can be used in the x- and y-axis orientation of the scanning sequence and another one is needed for the z-direction. For the z-direction, a simple open saddle core coil is used.

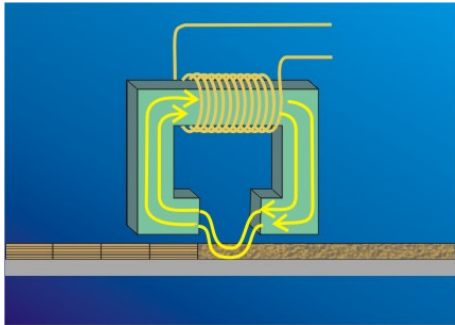


Figure 2 - Recording head magnetic flux

The flux inducing coils need to be characterized e.g. in the frequency range 10 Hz to 1 MHz, considering both the motion related frequencies as well as the switching frequency harmonics of the pulse width modulated drivers used to drive the actuators, linear and rotating motors. The characterization can be done by applying the probes over a micro-strip PCB structure of which the strip itself is narrow enough to capture the flux between the strip and the ground layer underneath, 1,6 mm apart [3].

Different from the RF applications, the strip line doesn't need to be matched to 50 Ω as the maximum frequency dealt with is 1 MHz and the calibration structure is just a simple Eurocard size FR-4 160 x 100 mm PCB. The mutual coupling effect between the sensing micro-strip wire and the flux injecting coils shall be minimized for which the strip over the ground layer is loaded by 50 Ω at the opposite sides of the board, see figure 3.

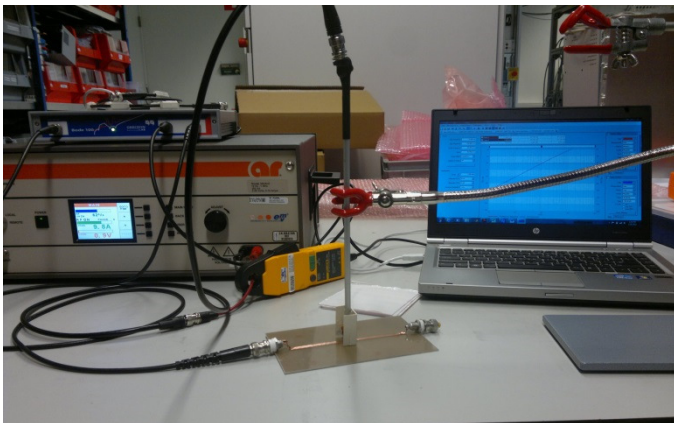


Figure 3 - H-field injection probe over a micro-strip test board

The LF current necessary to achieve sufficient H-field at the probe's gap at a small distance is limited to about 10 Amps, being the upper limit for the LF power amplifier used. Opposite,

at the higher frequencies the inductance of the probe becomes much higher than 50 Ω which make it difficult to drive current into the probe [4]. By means of a closed-loop feed-back circuit, the LF current driven into the injection probe is kept constant over frequency and is normalized against the response of the system. Measurements have indicated that the probe's induced voltage, in particular at the higher frequencies is determined by the strip or wire width of the micro-strip structure, see figure 4a and 4b.

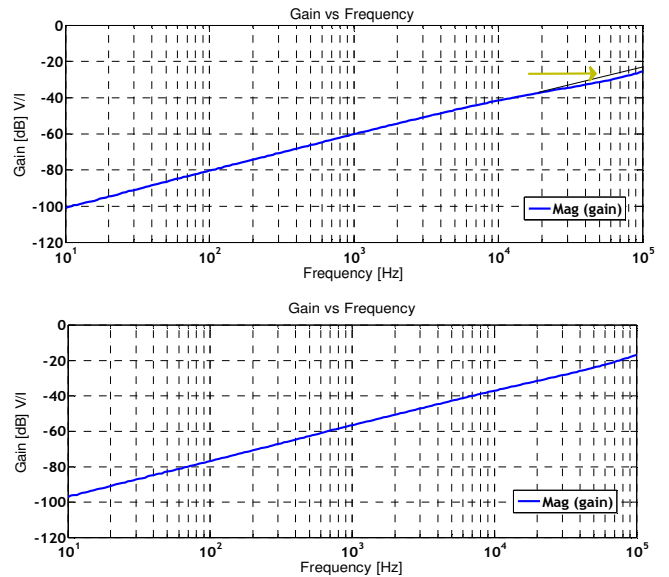


Figure 4 – Calculated transfer function versus measured transfer function. a) Wide strip b) Thin wire

When the frequency dependent transfer functions from the probes are known one needs to verify the linearity of the probe while driving it with high current. Furthermore, one needs to consider that the LF power amplifier used is not ideally linear too. While generating e.g. a 1 kHz H-field at several milli-Tesla (mT), multiple harmonics are generated too which may also affect the response of the sensor system used, see figure 5.

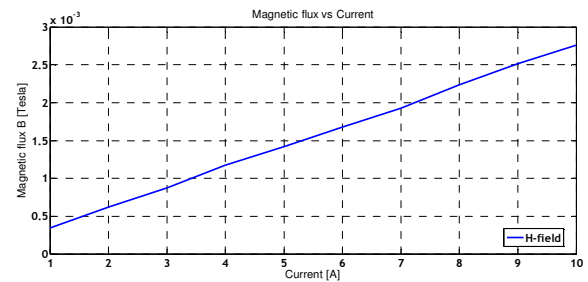


Figure 5 - Injection probe linearity

### III. SENSOR SYSTEM RESPONSES

Due to the H-field applied (with its harmonics) the sensor (or other subsystem) will respond as a voltage will be induced as well as multiple inter-modulation distortion (IMD) products. With an analogue sensor system it will be hard to determine the sensor's inter-modulation response from the coinciding LF

power generator harmonics. With a switching e.g. chopping amplifier or sampling sensor system with ADC the LF H-field disturbance will cause various IMD products which will add and subtract to all frequencies used. Instead of just looking at the prime response i.e. global indication of the sensor system, the entire analogue signal frequency band prior to discretization is considered as it will show the root cause for certain susceptibility issues. Long before the sensor's output signal becomes fully disturbed, small deviation can be detected from the frequency spectrum information often more than 100 dB deep, see figure 6.

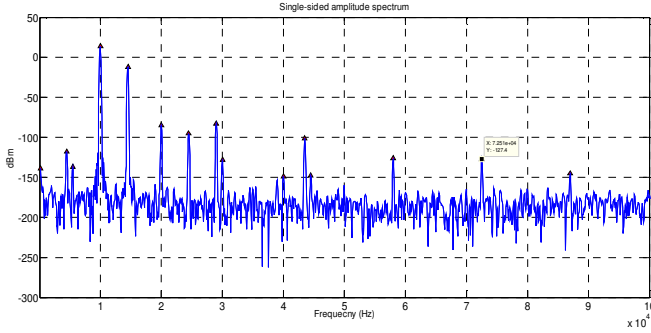


Figure 6 - A typical response of an analogue system

#### IV. MATHEMATICAL DERIVATION OF IMD

The usable dynamic range of an amplifier is limited at very small signal levels by the noise floor and at large signal levels by interference between signal frequencies. Distortions are caused by non-linearity in the amplitude transfer characteristics as a results produces harmonics. IMD results from the mixing of two or more signal at different frequencies. The output occurs at sum and difference of integer multiple of the input frequencies [5]. The non-ideal characteristics of an amplifier can be described by using the power series expression:

$$V_{OUT} = K_0 + K_1(V_{IN}) + K_2(V_{IN})^2 + K_3(V_{IN})^3 \quad (1)$$

An input signal:  $V_{IN} = E_1 \sin(\omega_1 t) + E_2 \sin(\omega_2 t)$  produce harmonic distortion, two input signal produces harmonic distortion and intermodulation distortion.

$$V_{IN} = E_1 \sin \omega_1 t + E_2 \sin \omega_2 t \quad (2)$$

Combining both equations (1) & (2) gives as follow:

$$V_{OUT} = K_0 + K_1(E_1 \sin \omega_1 t + E_2 \sin \omega_2 t) + K_2(E_1 \sin \omega_1 t + E_2 \sin \omega_2 t)^2 + K_3(E_1 \sin \omega_1 t + E_2 \sin \omega_2 t)^3 \quad (3)$$

The first term ( $K_0$ ) represents the DC offset of the amplifier, the second term is the output signal of the DUT. The subsequent terms represent the distortion of the amplifier. The second IMD can be found by analyzing the third term of equation (3).

$$K_2(V_{IN})^2 = K_2(E_1^2 \sin^2 \omega_1 t + E_2^2 \sin^2 \omega_2 t + 2E_1 E_2 (\sin^2 \omega_1 t (\sin \omega_2 t))) \quad (4)$$

Remembering that  $[\sin^2 x = (1 - \cos 2x)/2]$  and  $[\sin(x) \sin(y) = (\cos(x - y) - \cos(x + y))/2]$  and substituting into equation. (4).

$$K_2(V_{IN})^2 = \frac{K_2(E_1^2 + E_2^2)}{2} \dots \quad (5a)$$

$$\left(\frac{K_2}{2}\right) (E_1^2 \cos 2\omega_1 t + E_2^2 \cos 2\omega_2 t) + \dots \quad (5b)$$

$$2K_2 E_1 E_2 (\cos(\omega_1 t - \omega_2 t) - \cos(\omega_1 t + \omega_2 t)) \quad (5c)$$

The first and second terms in equation (5) represent DC offset and second-order harmonics. The third term represents second-order IMD. This exercise can be repeated with the fourth term of equation (3) to know about third-order effects.

$$K_3(V_{IN})^3 = K_3(E_1^3 \sin^3 \omega_1 t + E_2^3 \sin^3 \omega_2 t + 3E_1^2 E_2 \sin^2 \omega_1 t (\sin \omega_2 t) + 3E_1 E_2^2 \sin^2 \omega_1 t (\sin^2 \omega_2 t)) \quad (6)$$

Remembering that,  $\sin 3x = 1/4(3\sin x - \sin 3x)$  and  $\sin^2 x \sin y = 1/2(\sin y - 1/2(\sin(2x + y) - \sin(2x - y)))$ , equation (6) reduces to:

$$K_3(V_{IN})^3 = \left(\frac{3K_3}{4}\right) (E_1^3 \sin \omega_1 t + 2E_2^3 \sin \omega_2 t + 2E_1^2 E_2 \sin \omega_2 t + 2E_2^2 E_1 \sin \omega_1 t) \quad (7a)$$

$$(K_3 E_2^3 / 4) (E_1^3 \sin 3\omega_1 t + E_2^3 \sin 3\omega_2 t) + \quad (7b)$$

$$K_3 E_1^2 E_2 / 2 (\sin(2\omega_1 t - \omega_2 t) - 1/2 \sin(2\omega_1 t + \omega_2 t)) + \quad (7c)$$

$$K_3 E_2^2 E_1 / 2 (\sin(2\omega_2 t - \omega_1 t) - 1/2 \sin(2\omega_2 t + \omega_1 t)) \quad (7d)$$

Equation (7a) represents amplitude offset at the fundamental frequencies. Term (7b) signifies the third-order harmonics and term (7c) and (7d) represents third order IMD.

In addition, while driving the magnetic flux applied, the (non-) linear response to the LF H-field disturbance can be analyzed and extrapolation to higher flux intensities can be derived without the need to apply these often excessive fluxes. Close to the pole heads of a linear or rotating motor fluxes up to 1 Tesla and above can be found. Saturation of ferrite core materials starts from 300 mT or even less.

#### V. TOTAL SCAN SYSTEM

The total LF H-field scan system comprises a LF signal source, typically non-amplitude modulated, a LF power amplifier, a LF current probe (to measure the current driven into the injection probe) the field injection probe, a computer controlled x-/y-/z-table, a high resolution oscilloscope (with spectrum analyzer functionality) and a sensor target with its accompanying supply and excitation sources and (if necessary) readout, see figure 7.

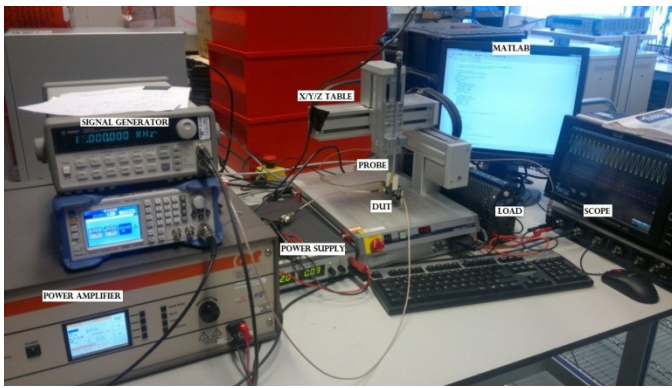


Figure 7 - Total LF H-field immunity test system

The H-field injected probe is mounted at table top surface scanner. As a device under test (DUT) an audio amplifier is used which is attached to surface scanner table as shown in figures 7 and 8. The scanning system is then able to derive the H-field sensitivities in the x-, y- and z-direction whereas the highest H-fields can only be generated in the x- and y-direction due to the recording head concept used with the field injection probe. At the output of the DUT, the various frequency inter-harmonic frequency components can be captured and put into a 2D plot for the two (or 3) field orientations. Thereafter, the full surface LF H-field sensitivity plots can be composed for each of the frequencies used. An example of a sensitivity plot at one of the inter-harmonics is given in figure 9.

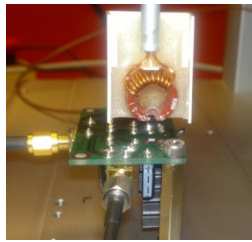


Figure 8 - Measuring in x-direction

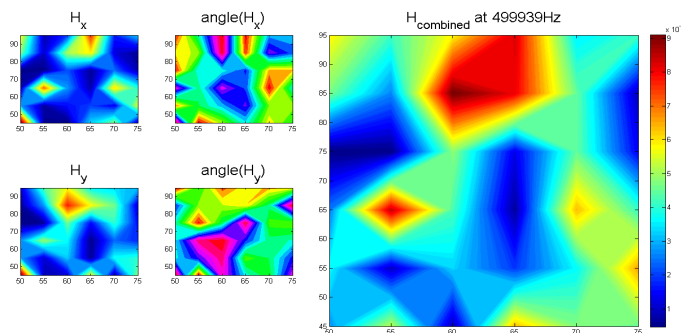


Figure 9 - LF H-field sensitivity plot

The response data can be used in graphical representation that allows the user to gain more insight into the behavior of electromagnetic field coupled into the scanned area i.e. DUT.

As can be seen from figure 9, also the phase relation between the sensor's excitation frequency and the LF-H-field disturbance can be adjusted yielding that the sensor's response vectors can be added accordingly rather than using the scalar output amplitudes.

## VI. CONCLUSIONS

Considering that (RF) emission and immunity surface scanning techniques are well-known and are COTS available, the constraints for building a sound LF H-field immunity test system has been large w.r.t. to:

- The H-field injection probe design (bandwidth: 10 Hz to 1 MHz, self-heating and resolution issues)
- The (non-)linearity of the LF power amplifier
- The calibration and characterization process for the H-field injection probe
- The frequency domain analysis method developed to derive the sensor's response long before the sensor's output signal becomes noticeable affected

The LF H-field sensor scanning has revealed that most sensors and other (amplifying) subsystems are susceptible over a wide range of disturbance frequencies and the sensor's (and other subsystems) response is affected by frequencies beyond the sensor's (and other subsystems) operational bandwidth.

The LF H-field surface scan method can be useful to detect and improve sensor designs or can be used to distinguish i.e. select between sensor suppliers. It is obvious that the sensor's immunity targets which have to be satisfied need to be known for the target position where the sensor will be placed.

This scanning method using one disturbance frequency signal at a time is not suited to forecast broadband interference signals though phase correlation between some sensors investigated and the LF H-field disturbance applied can be used when well chosen.

## ACKNOWLEDGMENT

The author and co-author (fulfilling his MSc assignment at Manipal University during his internship) wishes to thank ASML, Veldhoven for the collaborative work. The work has furthermore been supported by the Dutch Government (RVO) by the WBSO program under the Smesi project agreement.

## REFERENCES

- [1] [http://en.wikipedia.org/wiki/Electromagnetic\\_compatibility](http://en.wikipedia.org/wiki/Electromagnetic_compatibility)
- [2] [IEEE paper A Resonant Method to Construct Core Loss of Magnetic Materials Using Impedance Analyzer](#)
- [3] <http://www.cvel.clemson.edu/pdf/EMCS02-589.pdf>
- [4] [http://www.omicon-lab.com/fileadmin/assets/customer\\_examples/Experimental\\_Article-Coupling\\_between\\_Cylindrical\\_Coils.pdf](http://www.omicon-lab.com/fileadmin/assets/customer_examples/Experimental_Article-Coupling_between_Cylindrical_Coils.pdf)
- [5] <http://www.ti.com/lit/an/sboa077/sboa077.pdf>